Construction of vascularized tissue-engineered breast with dual angiogenic and adipogenic micro-tissues

Ruopiao Ni [a,b,c,1], Chao Luo [a,b,1], Hai Ci [a,b], Di Sun [a,b], Ran An [a,b], Zhenxing Wang [a,b], Jie Yang [a,b,**], Yiqing Li [c,***], Jiaming Sun [a,b,*]

[a] Department of Plastic Surgery, Union Hospital, Tongji Medical College, Huazhong University of Science and Technology, 1277 Jiefang Avenue, Wuhan, 430022, China
[b] Wuhan Clinical Research Center for Superficial Organ Reconstruction, Wuhan, 430022, China
[c] Department of Vascular Surgery, Union Hospital, Tongji Medical College, Huazhong University of Science and Technology, Wuhan, China

ARTICLE INFO

ABSTRACT

Hydrogel-based micro-tissue engineering technique, a bottom-up approach, is promising in constructing soft tissue of large size with homogeneous spatial distribution and superior regeneration capacity compared to the top-down approach. However, most of the studies employed micro-tissues with simple mesenchymal stem cells, which could hardly meet the growth of matrix and vessels. Therefore, we recommend a dual micro-tissues assembly strategy to construct vascularized tissue-engineered breast grafts (TEBGs). Adipose micro-tissues (AMs) and vessel micro-tissues (VMs) were fabricated by seeding adipose-derived stem cells (ADSCs) and human umbilical vein endothelial cells (HUVECs) on collagen microgels (COLs) with a uniform diameter of ~250 μm, respectively. TEBGs were constructed by injecting the dual micro-tissues into 3D printed breast-like Thermoplastic Urethane (TPU) scaffolds, then implanted into the subcutaneous pockets on the back of nude mice. After 3 months of implantation, TEBGs based on dual micro-tissues performed larger volume of adipose tissue regeneration and neo-vessel formation compared to TEBGs based on single AMs. This study extends the application of micro-tissue engineering technique for the construction of soft grafts, and is expected to be useful for creating heterogeneous tissue constructs in the future.

1. Introduction

Breast defects caused by mastectomy, trauma or congenital malformations adversely affect patients' physical and mental health. Current surgical treatments are often companied with donor-site morbidity, immunological reaction or inflammatory response [1,2]. Tissue-engineered breast graft (TEBG), using autologous stem cells extracted from a small amount of tissue and expanded in vitro, is very promising for breast reconstruction with less trauma and lower immunogenicity [3]. The traditional TEBG involving a top-down approach [4] is fabricated by seeding stem cells on pre-fabricated integrated scaffolds

and adding specific growth factors [5]. Although great progress has been made, it is difficult to build TEBG with large volume due to the following reasons: 1) Dispersed seeding cells in large scaffold after cultivation in monolayer, digestion and resuspension consequently results in insufficient cell-to-cell connection and short of ECM deposition [6]. 2) Lack of nutrients and poor oxygen exchange in the middle area of the scaffold, further resulting in necrosis and uneven distribution of cells [7,8]. 3) It is difficult to provide a tissue-specific microenvironment and mimic the natural complex architecture in a micro-scale.

Inspired by the unit-repetitive module of native tissues (such as osteon for bone), a bottom-up approach was proposed to build a large

---

volume of tissue constructs by assembling modular micro-tissues [9]. Micro-tissues are clusters of cells and extracellular matrix (ECM) excreted by the cells, comprising self-assembly multicellular aggregate and cell-biomaterial assemblies [10], which have the following superiorities: 1) Precultured micro-tissues with high cell density have tighter intercellular connection and manufacture more ECM compared to dispersed cells. 2) Micro-tissues technology is potential to overcome the obstacle of nutrition and metabolism by facilitating nutrient diffusion through pores among micro-tissues in early-stage and ingrowth of blood vessels from the host in the later period. 3) With assistance of several micro-fabrication technologies such as micro-molds [11], electrospinning technology [12], microfluidics [13], and PDMS chips [14], cells aggregate into micro-tissue with a specific geometric form as needed, readily mimic basic unit of specific organ tissue [15]. And the functionally alterable components, such as collagen and so on, can provide cell chemical microenvironment. Different micro-tissues can act like modules to assemble complex and multi-component tissue.

Adipose-derived stem cells (ADSCs) are commonly used for constructing adipose micro-tissues due to its abundant source, accessibility, and low immunogenicity [16]. Hoefner, C and co-workers cultured ADSCs spheroids and found that their ECM mainly consisted of fibronectin, collagen V, and VI and shifted into laminin, collagen I, IV, V and VI after adipogenic induction in vitro, like ECM in native adipose tissue [17]. Some ADSCs micro-tissues were fabricated and lipid accumulation were observed in vitro [18–20]. However, when it comes to animal experiments, single adipose micro-tissues are easy to result in adipose tissue atrophy and fibrosis due to insufficient vascularization [18].

Native breast is mainly composed of vascularized adipose tissue [21]. In intact adipose tissue, adipocytes account for 14.6% and vascular-associated cells for 70%, with adipocytes clustered and surrounded by vascular-associated cells [22]. The adipogenesis (regeneration of adipose tissue) and angiogenesis (sufficient vascular supply) are interdependent. Adipocytes in adipose tissue need the capillary network to feed. Sufficient neo-vascularization can reduce the atrophy and fibrosis during the regeneration of adipose tissue by providing nutrient supply and recruiting surrounding cells [23]. Meanwhile, ADSCs in adipose tissue have the potential to facilitate the ingrowth of neo-vessel, stimulating endothelial cell proliferation, migration, total vessel length, the total number of junctions, and cell junction density by releasing IL-8, CCL-2, TIMP-1, TIMP-2, and VEGF [24,25].

In order to enhance vascularization, human umbilical vein endothelial cells (HUVECs) are commonly used in pre-vascularization. With the presence of supporting cells, HUVECs are expected to pre-form immature networks, develop, and even interconnect to the host blood vessels [26,27]. In vitro studies have shown that the co-culture of ADSCs and HUVECs induces the formation of vascular networks on 3D constructs [28], yet monoculture of ADSCs or HUVECs on collagen or 2D environment without exogenous growth factor failed to form vessel-like structure neither in vitro nor in vivo [29]. Though Sarkanen J induced tubule network formation in monoculture of ADSCs with exogenous growth factors, they found ADSCs combined with HUVECs presented remarkable enhancement in capillary formation and maturation [30]. Yao, R developed micro-tissues by coating adipogenic-induced ADSCs/collagen/alginate microspheres with collagen and HUVECs. After subcutaneous injection of micro-tissues for 12 weeks, obvious adipose tissue regeneration stained with Oil red O and sparse vasculature were observed [31]. Therefore, we suggest that using ADSCs and HUVECs to culture dual micro-tissues as adipogenic and angiogenic building blocks may be a novel strategy for breast tissue engineering.

In the present study, TEBG with enhanced adipogenesis and angiogenesis was constructed by assembling dual micro-tissues, adipose micro-tissues (AMs) based on ADSCs and vessel micro-tissues (VMs) based on HUVECs, in a 3D printed breast scaffold (Fig. 1). The collagen microgels (COLs), with a uniform diameter of ~250 μm and high compatibility, were prepared from a water-in-oil microfluidic chip and EDC/NHS crosslinking to act as micro-carriers for cells. In vitro expansion and

differentiation of ADSCs was followed by injecting AMs and VMs into 3D-printed TPU scaffolds to fabricate TEBG. Last but not least, we investigated lipogenesis and angiogenesis in vivo.

2. Materials and methods

2.1. Preparation and characterization of COLs

2.1.1. Fabrication of microfluidic chip

Circle glass capillary with inner diameter of 100 μm was inserted into another circle glass capillary with inner diameter of 500 μm and then fixed on a glass slide using glass glue to make a microfluidic chip with co-flow structure. Tip of 10 μl was assembled on the top of inner capillary as injector port of dispersed phase, and tip of 200 μl was assembled on the top of outer capillary as injector port of continuous phase.

2.1.2. Preparation of COLs

COLs were prepared by a capillary-based microfluidic chip. Type I collagen (Kele, Chengdu, China) was dissolved in 0.1 M acetic acid (Sinopharm Chemical ReagentCo., Ltd) and collagen solution was passed into the inner layer as dispersed phase. N-decyl alcohol containing 5% (v/v) Span80 was passed into outer layer as continuous phase. Then collagen micro-droplets forming in capillary were passed into crosslinker solution through silicon hose. The crosslinker solution was composed of 50mgEDC (Sigma-aldrich, Darmstadt, Germany), 20 mg NHS (Sigma-aldrich, Darmstadt, Germany), 500 μl tween-20 (Solarbio, Beijing, China) and 10 ml Tris-HCl-NaCl (52.596 g NaCl and 10 ml 1 M Tris-HCl buffer diluted to 200 ml with deionized water). After 24-h crosslinking, COLs were washed by 95% ethanol for 3 times and collected in water.

2.1.3. Cell seeding efficiency

Every 10 μl cell suspension (10^7 cells/ml) was seeded on 10 μl COLs and medium was added to 100 μl 2 h later. CCK8 assay was tested after 24 h. According to the standard curve, calculate the cell count N. Cell seeding efficiency = $N/10^5*100\%$

2.1.4. Porosity

COLs were fixed using 2.5% glutaraldehyde for 4 h and washed using PBS for 3 times. After gradient dehydration with serial concentrations of ethanol, COLs were freeze-dried for 24 h and weighed. After recording the dry mass as M1 mg. Immerse the dry COLs in 75% ethanol for 24 h, weigh the wet mass as M2 mg and measure their volume as V ml. Calculate porosity= (M1-M2)/(0.85* V) *100%.

2.1.5. Particle size analysis

The particle size analysis was done using Laser particle size analyzer Mastersizer 2000 (Malvern, England). COLs of 1 ml were dissolved in 1 L water and then measured.

2.2. Construction and characterization of dual micro-tissues

2.2.1. Isolation and in vitro culture of human adipose-derived stem cells (ADSCs)

Adipose tissues were obtained from patients underwent abdominal liposuction. We isolated ADSCs according to method described by Zuk et al. Lipoaspirates were washed with saline and then digested by 0.1% (w/v) collagenase II (Solarbio, Beijing, China). 4 h later, collagenase was neutralized with an equal volume of low-glucose Dulbecco's Modified Eagle Medium (DMEM) (HyClone, Logan City, UT, USA) and suspension was centrifuged at 1500 rpm for 5 min. ADSCs were cultured in low-glucose DMEM containing 10%FBS (HyClone, Logan City, UT, USA) and 1% penicillin and streptomycin (ThermoFisher Scientific, Waltham, MA, USA). Digest ADSCs with 0.25% trypsin/1 mM EDTA (ThermoFisher Scientific) when ADSCs reached 80%–90% confluence and then passage. Passages 3 to 6 of ADSCs were used in all experiments.
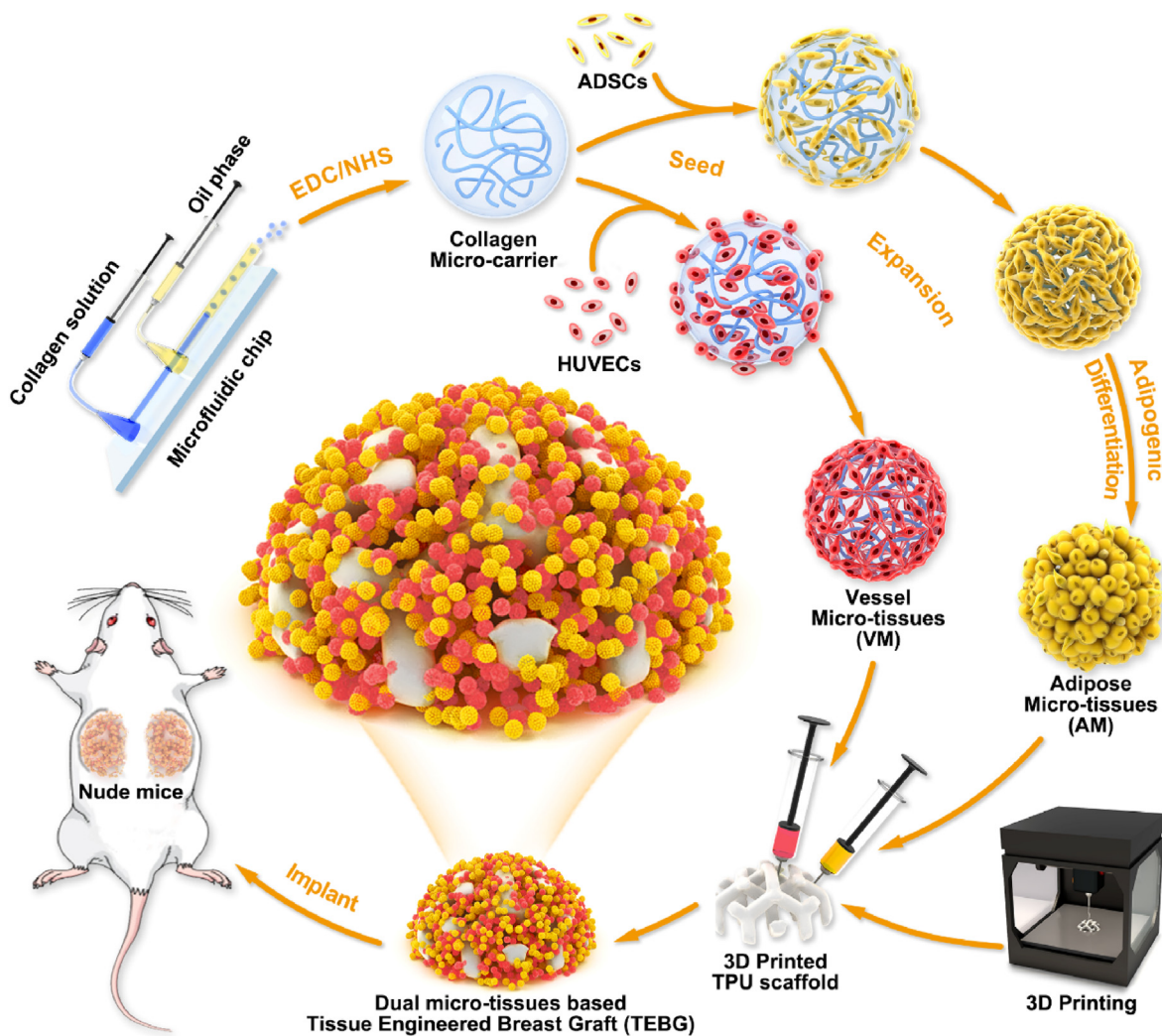
Fig. 1. Schematic diagram of the experiment. Tissue-engineered breast graft (TEBG) was constructed by assembling dual micro-tissues based on collagen micro-carriers (COLs). Firstly, collagen micro-droplets formed through microfluidic chip and were cross-linked by EDC/NHS to fabricate COLs. ADSCs and HUVECs were separately seeded on COLs and cultured to construct adipose micro-tissues (AMs) and vessel micro-tissues (VMs). After dynamic expansion and adipogenic differentiation, dual micro-tissues were assembled with 3D printed TPU scaffold to construct a tissue-engineered breast graft (TEBG) and transplanted under the skin of nude mice.

2.2.2. In vitro culture of human um-bilical vein endothelial cells (HUVECs)

HUVECs were purchased from Zhong Qiao Xin Zhou Biotechnology Co. Ltd (Shanghai, China). HUVECs were cultured in RPMI 1640 Medium (HyClone, Logan City, UT, USA) containing 10%FBS.

2.2.3. Construction of adipose micro-tissues (AMs) and adipogenic induction

Prior to seeding cells, COLs were sterilized by soaking in 75% ethanol 30min for 3 times. Remove the ethanol and coat COLs with 0.1% gelatin solution at constant temperature of 37 °C overnight. ADSCs at passage 3 were digested with trypsin and resuspended with low-glucose DMEM medium at a cell concentration of 10^7 cells/ml. Every 100 μl COLs were seeded with 100 μl cell suspension at 37 °C. 2 h later, add low-glucose DMEM medium to 5 ml along the wall of test tube slowly. Change the medium every 3 days. 7 days later, change the low-glucose DMEM into adipogenic induction medium (DMEM-high glucose supplemented with $10{-}7$ M dexamethasone, 50 μg/mL L-ascorbate-2-phosphate, 10 μg/ml indomethacin, 10% FBS, and 1% penicillin/streptomycin). COL-ADSCs were adipogenic induced for 14 days to construct AMs.

2.2.4. Construction of vessel micro-tissues (VMs)

In addition to replacing low-glucose DMEM medium with RPMI-1640 medium, COLs and HUVECs were disposed as mentioned above. Isolated HUVECs were calculated and seeded on 0.1% gelatin-coated sterilized COLs with a cell concentration of 10^6 cells. Change the RPMI-1640 every 3 days and culture COL-HUVECs for 7 days to construct VMs.

2.3. In vitro biocompatibility assessment

2.3.1. CCK-8 assay

To evaluate the cell viability of ADSCs and HUVECs when 3D cultured on COLs, CCK-8 assay was performed in 96-well plate plated with 5% agarose. 10 μl COLs and 10^5 cells were added into each well. Change the medium every 3 days. At the specific time point (0 h, 12 h, 3d, 7d, 14d) after seeding cell, remove the micro-tissues into another 96-well plate and soak up the liquid. According to the manufacture's protocol, micro-tissues were mixed with 100 μl medium and 10 μl Cell Counting Kit 8, then incubated in 37 °C 5%CO2 in dark for 4 h. The optical density (OD)

was measured at 450 nm with spectrophotometer (ThermoFisher Scientific Corporation, USA).

2.3.2. Live/dead assay

The cell viability of ADSCs and HUVECs on COLs was further determined by Calcein acetoxymethyl ester/propidium iodide (Calcein-AM/PI) staining. At the specific time point (1d, 4d, 7d) after seeding cells, micro-tissues were washed 3 times with PBS and treated with Calcein-AM at 37 °C for 35min. Then micro-tissues were immersed in growth medium at 37 °C for 30min to get the live cells converse Calcein-AM into Calcein (green fluorescence). Remove the growth medium and then micro-tissues were incubated with PI for 5min. The living cells with green fluorescence and dead cells with red fluorescence were observed by confocal microscope.

2.3.3. Environment scanning electron microscopy (ESEM) analysis

ESEM analysis was performed to observe the surface of COL and cell spreading on COL. COLs or micro-tissues were fixed in 4% (v/v) glutaraldehyde and then dehydrated with serial concentrations of ethanol (50%,70%,80%,90%). After dried in air and sputtered with gold, the surface of COL, morphology of ADSCs and HUVECs on COLs and the ECM cells excreted were observed by ESEM (Quanta200, FEI, Holland).

2.3.4. Oil Red O staining

After ADSCs were seeded on COLs for several days (0day, 7days, 14days and 21days), Oil Red O staining (ORO) were performed according to manufacturer's manual (Solarbio G1262, Beijing, China). Micro-tissues were fixed with ORO fixative for 15min and then washed with distilled water for 2 times. After soaking samples with 60% isopropanol for 5minm, discard it and add the prepared ORO Stain (ORO stain A; ORO stain B = 1:1) 0.10–20min later, wash samples for 3 times and observe with optical microscope.

2.3.5. Quantitative reverse transcription PCR (qRT-PCR)

Total RNA was isolated from ADSCs with the RNeasy Mini Kit (QIAGEN). Reverse-transcription was performed using SuperScript III Reverse Transcriptase (Invitrogen, Tokyo, Japan) and random primers (Invitrogen) according to the manufacturer's guidelines. cDNAs were used for PCR utilizing Platinum SYBR Green qPCR SuperMix UDG (Invitrogen). PPARγ and CEBP expression levels were normalized to an endogenous control, GAPDH. The sequences of the GAPDH, PPARγ and CEBP primers (Invitrogen) were as follows (Table 1).

2.4. Assembly of tissue-engineered breast graft（TEBG）in vitro

2.4.1. Fabrication of breast-like scaffolds

The breast-like scaffold model was designed using UG NX10.0 (Siemens PLM Software, USA) transformed into STL model, and then imported into slicing softwares Cura 15.02 (Ultimaker, Netherlands) to produce 3D printer recognizable Gcode files. The details of architecture design could refer to our previous study. The scaffolds were 3D printed by Fused Deposition Modeling (FDM) Printer (Allcct, Wuhan, China) using Thermoplastic Urethane (TPU) filaments (eFlex, ESun, Shenzhen, China). The layer thickness, feed rate and extrusion temperature were

respectively set to 0.1 mm, 40 mm min−1 and 210 °C. The TPU scaffolds were observed under Stereo Microscope (Nikon, Japan).

2.4.2. Assembly of TEBGs

Dual micro-tissues (AMs and VMs) were assembled with TPU breast-like scaffold by pumping. Prior to assembly, TPU scaffolds were sterilized through ethylene oxide and then immersed in 2% Chitosan solution overnight. Then AMs and VMs were separately loaded in syringe (1 mL) with needle of 19 gauge and pumped into scaffold by syringe pump with the even pump speed (2.5 mm/min) at the same time. Every 30s, the scaffold was rotated 90° clockwise. Within 2 min, each tissue-engineered breast model was filled with 100 μl AMs and 100 μl VMs.

2.5. Animal experiment

2.5.1. Animal

Female NU/NU nude mice (8 week, 20–25 g) were purchased from Vital River (Beijing, China). This study was approved by the animal ethics committee of Tongji Medical College, Huazhong University of Science & Technology (Wuhan, China). Sacrifice of animals was consistent with state regulations and laws and in accordance with the Standing Committee on Ethics in China (State Scientific and Technological Commission of China). The protocol was approved by ethical committee (approval number: 2019-S069).

2.5.2. Experimental procedure

24 nude mice were used as animal model and randomly divided into four groups: ①Blank: TPU scaffold ②COL: TPU scaffold + COLs ③AM:TPU scaffold + AMs ④AM + VM: TPU scaffold + AMs + VMs. Nude mice were anesthetized with 4% Chloral hydrate by Intraperitoneal injection. A dorsal midline incision of 2 cm was made. The skin was mobilized by blunt dissection to make two subcutaneous pockets and two TEBGs were separately placed in the left and right pockets. The incision was stitched up with 3–0 suture and sterilized with 1% povidone-iodine.

2.5.3. Magnetic resonance imaging (MRI)

12 weeks after transplantation, TEBGs were harvested and subjected to magnetic resonance imaging (BioSpec 70/20USR, Bruker, Germany). An MRI research system with the field strength of 7 T was used to conduct this analysis. The scanning parameters were set as follow: TR = 4000 ms, TE = 36 ms, slice thickness = 1 mm, FOV = 7cm × 7 cm, matrix size = 256 × 256.

2.6. Histology & immunofluorescence analysis

2.6.1. Hematoxylin and eosin staining

After 12 weeks of transplantation, TEBGs were fixed with 4% paraformaldehyde and embedded in paraffin. A standard staining of hematoxylin and eosin was performed.

2.6.2. Perilipin staining

Perilipin positive cells were counted in randomly 5 area at 200× magnification.

2.6.3. CD31 and Ki67 staining

CD31 expression was observed in the cytoplasm and cell membranes of endothelial cells of dermal micro-vessels. The sections were first scanned at low power (x40) to identify the hot-spots (areas of highest micro-vessels density [MVD] count). Afterward, five non-overlapping random areas were examined under ×200 magnification (0.09 mm), and the sum of micro-vessels count was recorded.

2.7. Statistical analyses

Experiments in vitro were repeated 3 times independently with cells of same passage. Statistical analyses were performed with Prism5.

Table 1
Primers sequences used for qRT-PCR.

Gene	Primer	Sequence (5′-3′)	PCR Products
Homo GAPDH	Forward	TCAAGAAGGTGGTGAAGCAGG	115bp
	Reverse	TCAAAGGTGGAGGAGTGGGT	
Homo PPARγ	Forward	GACCACTCCCACTCCTTTGA	242bp
	Reverse	ATGAGGGAGTTGGAAGGCTC	
Homo CEBP	Forward	ACTCGTTGCTGTTCTT	496bp
	Reverse	ACCAGTGACAATGACC	

Independent *t*-test was carried out to compare the results of two groups and one-way ANOVA was performed to proceed multiple group comparisons. Values were present with mean ± standard deviation (SD) and statistical significance was considered when P < 0.05.

3. Results

3.1. Fabrication and characterization of COLs

Initially, we fabricated micro-carriers for seeding cells through microfluidic technology. Collagen solution passed into a microfluidic chip as a dispersed phase was sheared by a continuous oil phase into collagen droplets continuously and evenly, and maintained stability with the presence of surfactant Span80 (Fig. 2A and B). As a result of Span80 and Tween 20 in cross-linker solution, droplets remain stable until they are crosslinked into COLs (Fig. 2C). The COLs are microspheres with a smooth surface (Fig. 2D and E). We used COLs of around 250 μm for the reason that nutrients can diffuse only within ranges of 100–200 μm. The particle size analysis confirmed an even distribution of COLs in size and adequate stability (Fig. 2F).

The COLs were prepared in different collagen concentrations (1%, 2% and 4% w/v). The high collagen concentration reduces the porosity of COLs (2% vs 4%, P < 0.05) (Fig. S1). Next, the seeding efficiency of cells was evaluated. ADSCs and HUVECs adhered to COLs in 2 h with rounded morphology, and COLs demonstrated excellent cell spreading and proliferation within 32 h (Fig. S2). The results indicate that higher collagen concentrations facilitate cell adhesion and improve seeding efficiency (1% vs 2%, P < 0.01) (Fig. S1). Therefore, we prepared COLs with 2% collagen concentration for the follow-up experiment. FT-IR results of COLs confirmed collagen characteristics peaks at a wavenumber about 1634 cm−1 for amide I (C═O stretching), 1539 cm−1 for amide II (N–H deformation), 1235 cm−1 for amide III (tertiary C–N stretching vibration), 3289 cm−1 (amide A; N–H stretching) and 2931 cm−1 (amide B; C═O stretching) (Fig. 2G).

COLs demonstrated their suitability as carriers of ADSCs and HUVECs. The cytocompatibility of COLs with ADSCs and HUVECs was performed using a CCK8 assay. The proliferation of ADSCs and HUVECs on COLs reached a peak after seven days, and then a plateau phase in the proliferation curve was observed (Fig. 2H and I).
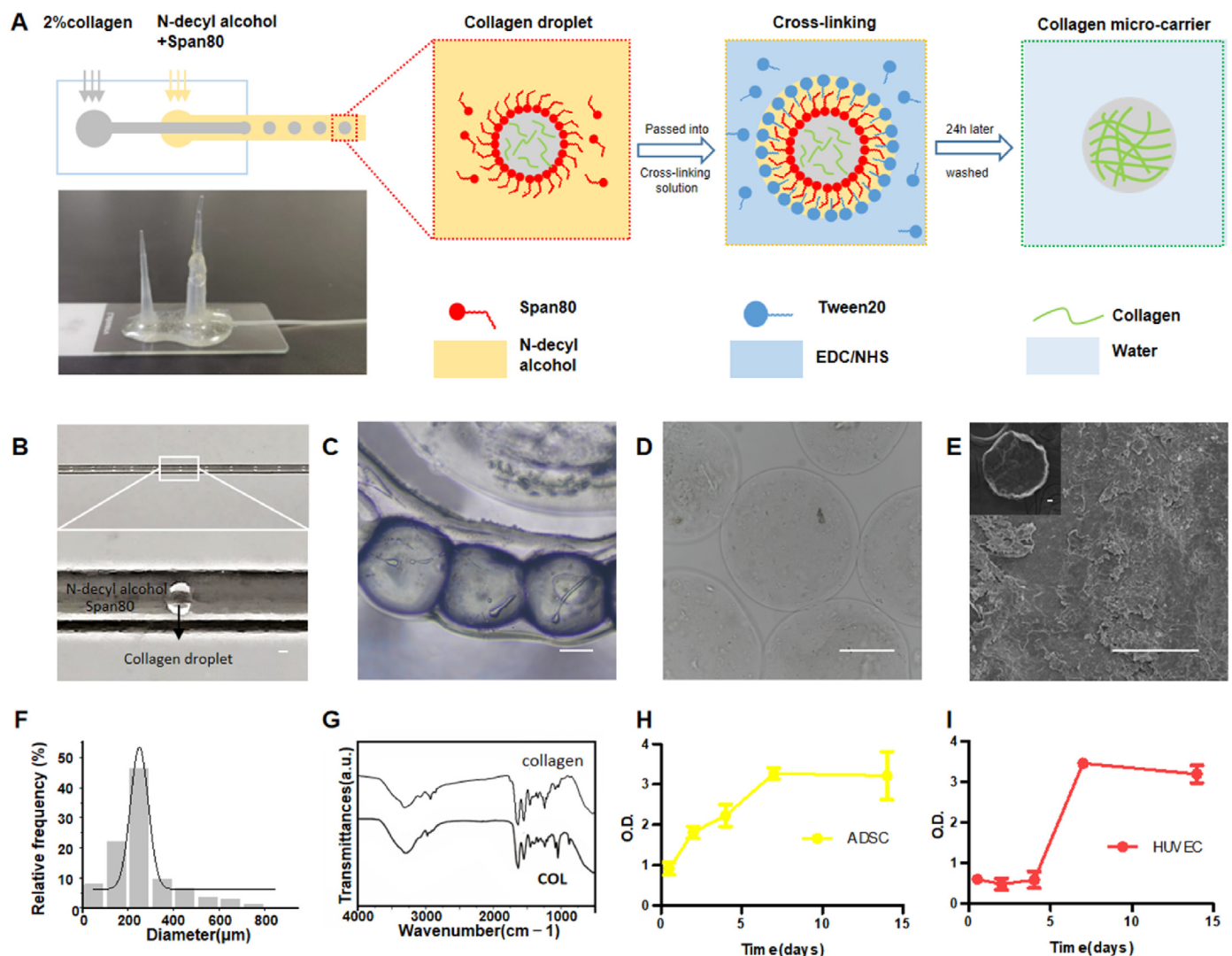

Fig. 2. Fabrication and Characterization of COLs. The schematic illustration of microfluidic-based COLs fabrication (A). Collagen droplets formed in microfluidic chips (B). Collagen microspheres in EDC/NHS (C) and crosslinked collagen micro-carriers in water (D) were observed under a light microscope. Surface morphology of COL was observed by SEM (E). The particle size analysis of COLs (F). FT-IR of COL showed the characteristic peak of collagen (G). CCK8 test of ADSCs and HUVECs on COLs (H, I). Scale bars in B&C&D, 100 μm. Scale bars in E, 10 μm.

3.2. Construction of AMs and VMs

According to the CCK8 assay, the first step to construct AMs or VMs was expanding ADSCs or HUVECs on COLs for seven days. Within 24 h after seeding cells onto COLs, Calcein-AM/PI shows a circle of cells sparsely adhered to the surface. Few dead cells can be observed with red fluorescence. ADSCs or HUVECs remained viable and exhibited steady growth until day seven (Fig. 3A). After day seven, AMs and VMs were spheroids containing high densities of live cells. Cracks between spherical micro-tissues may have been conducive to fluid infiltration and nutrient exchange, contributing to high cell viability. The SEM images show the gradual spread of ADSCs and HUVECs exhibiting pseudopodia and filopodia. The cells were round and appeared unattached on day one. On days four and seven, flattened and elongated cells and blurring cell boundaries were observed. Over time, the surface of the COL became rougher, signifying excretion and deposition of ECM (Fig. 3B).

Following cell expansion, AMs were further induced with adipogenic-specific culture conditions. Quantitative gene expressions were analyzed for AMs after 7, 14 and 21 days. PPAR-γ plays a significant role in regulating adipogenesis and maintaining differentiation. Therefore, PPAR expression increases during adipogenesis. During in vitro adipogenesis, PPAR-γ gene expression increased for the first 14 days before decreasing by the third week (Fig. 3D). A 5-fold increase in PPAR-γ expression was observed at the end of the 14th day of differentiation. Gene expression levels of C/EBP were similar to those of PPAR-γ (Fig. 3E). Compared to adicpogenesis differentiation in 2D (in a petri dish), 3D (AMs) had no adverse effects. Hence, AMs were cultured for 14 days in vitro to induce adipogenesis. Qualitative Oil Red O staining revealed a steady increase in lipid droplet accumulation during 14 days of in-vitro adipogenesis (Fig. 3C).

3.3. Assembly of dual micro-tissues

The AMs were collected after a 7-day cell expansion and a 14-day adipogenic differentiation period. VMs were collected after a seven-day cell expansion period (Fig. 4A Left). A phenomenon of aggregation was observed during the culture of AMs and VMs. Micro-tissues were initially dispersed in a culture medium. As for AMs or VMs collected, close micro-tissues connected and self-assembled to form larger constructs (Fig.4A, Fig. S3). The fusion of building blocks is a crucial and fundamental process in biofabrication. The physical contact between several micro-tissues will initiate the aggregation over time [32]. Cell-cell, cell-COL, and cell-matrix connections facilitated different micro-tissues' assembly. In vitro self-assembly of AMs and VMs showed that they could be used as building blocks. Due to the micro-scale, AMs and VMs were injectable.

Breast-like scaffolds were 3D printed to assemble with injectable building blocks. The software was used to design a semi-ellipsoid 3D model with a theoretical porosity of 85.7% (Fig. 4B). The printed TPU scaffold has a diameter of 1 cm and actual porosity of 80.96% (Fig. 4C). TPU scaffold was coated with chitosan for 24 h at 37 °C before assembly to enhance micro-tissues retention in scaffold. The AMs and VMs were loaded into 1 ml syringes and injected into the TPU scaffold using an injection pump (Fig. 4D). According to the method, TPU scaffolds were filled with dual micro-tissues, as shown in the photograph (Fig. 4E). Adipogenesis and angiogenesis were explored in vivo by implanting TEBGs under the dorsal skin of female nude mice (Fig. 4F).

3.4. TEBGs in vivo

3 months after implantation, TEBGs were integrated with nearby tissue. The samples of group AM and AM + VM seemed much plumper than those of group Blank and COL with naked eyes although the weight of samples had no statistical difference among groups (Fig. 5A and D). In group Blank and COL, there were many voids could be seen, and tissue was mainly white or gray colored fibrotic tissue. In contrast to that, yellowish fat-like tissue occupied a lot in group AM and AM + VM

(Fig. 5A). The MRI was taken to evaluate the volume of fat formation, which was present with high signal at T1W1 (Fig. 5B). According to cross-sectional diagram of MRI, there were barely fat regeneration in group Blank and COL. A wide range of adipose tissue could be found especially on the edge of scaffold. The volume calculated through the 3D reconstruction with MIMICs 21.0 were $1 \pm 1\%$, $18.80 \pm 2.58\%$, $29.5 \pm 1.66\%$ and $43.13 \pm 4.22\%$ respectively (Fig. 5E). However, MRI only indicated the bulky fat. HE staining was taken to further confirm formation of adipose tissue, fibrotic tissue and voids. The cross-section of TPU could be clearly observed in all groups, indicating that TPU scaffolds were not degraded yet in 3 months, and thin fibrotic tissue surrounding with TPU scaffold could be observed. However, TPU has been proven to be compatible and elastic, which is fit for soft tissue engineering [33]. Reddish COLs interspersed in tissue with the degradation on different levels. In COL group, COLs were not degraded completely as shown in cross-sectional HE staining with black star. However, few COLs could be observed in AM and AM + VM group. Several fat lobules and neo-vessels were observed in group AM and AM + VM (Fig. 5C). The quantitative analysis of HE staining reveals the significant proportion of adipose tissue and minimal fibrotic tissue proportion in the AM + VM group (Fig. 5F and G).

Perilipin immunofluorescence was used to mark lipid droplets in adipocytes. Similar to HE staining, perilipin (+) adipocytes in the Blank and COL group were significantly less than the AM + VM group. In group AM and group AM + VM, perilipin (+) cells were observed at both edges and in the middle of the scaffold (Fig. 6A and B). In addition, the perilipin (+) lipid droplets in the Blank and COL group appeared irregular and incomplete. The number of perilipin (+) adipocytes in group AM + VM was significantly higher than in group AM (188.9 ± 21.31 vs. 132.4 ± 9.980, P = 0.0182) (Fig. 6C). Out of four groups, AM + VM had the most significant percentage of perilipin (+) cells (Fig. 6D). The adipogenesis was further evaluated through relative gene expressions analysis of PPARγ, C/EBPα and FABP4. Gene expression levels of PPARγ and C/EBPα of group AM were higher than that of Blank and COL groups without any cell addition. 74-fold increase and 4-fold increase in PPAR-γ expression was observed in AM + VM compared with Blank and AM. Gene expression levels of C/EBPα and FABP4 in AM + VM also were highest in all groups (Fig. S4). The expressions of adiopogenic-related genes were consistent with histological results.

To evaluate the angiogenesis in vivo, CD31 and ki67 were immunofluorescence stained. Vessels are identified as CD31 (+) structures with visible lumen. Scattered CD31 (+) Ki67(+) cells showed some endothelial cells were proliferating (Fig. 7A).AM + VM had the highest number of CD31 (+) lumens at 200× magnification (23.5 ± 3.5) out of four groups (Fig. 7B). The average diameter of the vessels was similar among the four groups (Fig. 7C). The results of PECAM-1 expressions, also called as CD31, was consistent with the immunofluorescent staining of CD31. Angiopoietin-1 is secreted by vascular smooth muscle cells, which could promote endothelial cell sprouting and tissue invasion of new blood vessels. The angiopoietion-1 expression of AM + VM was highest in four groups (Fig. S4).

4. Discussion

In the present study, a TEBG was fabricated by assembling dual micro-tissues in a 3D printed breast scaffold to develop breast-like adipose tissue with adequate vascularization. Microgels were prepared by microfluidic method with the characteristics of high-throughput production, uniform particle size and good biocompatibility, as carriers for ADSCs and HUVECs to construct adipogenic and angiogenic micro-tissues. The ratio and position of dual micro-tissues in TEBG could be controlled to mimic breast structure. The TEBG with AMs and VMs had better adipose regeneration and neovascularization effects than AMs only.

The COL prepared by microfluidics method has the characteristics of high-throughput production, uniform particle size and good
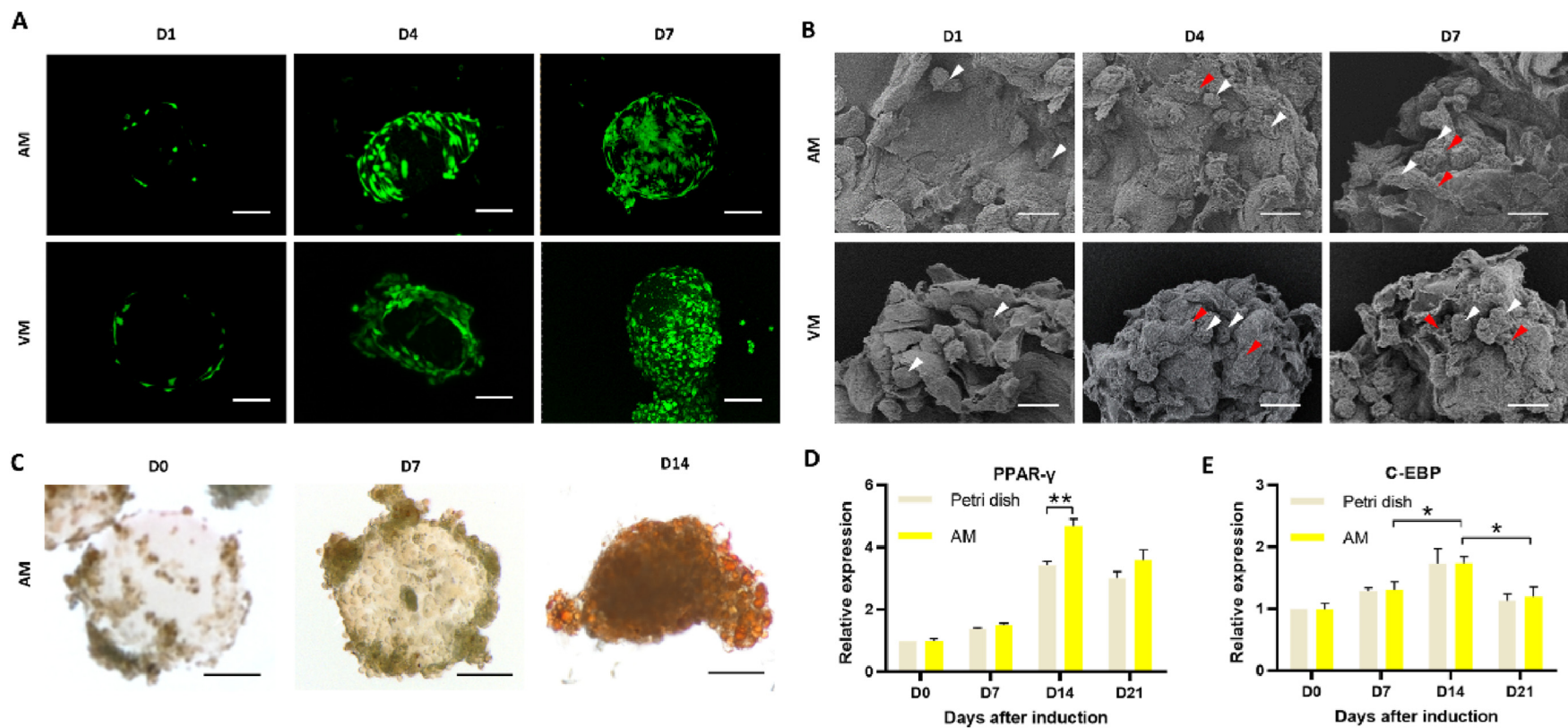
Fig. 3. Construction of AMs and VMs. ADSCs and HUVECs seeded on COLs were kept alive and proliferated (A) after one day, four days, and seven days. The ESEM showed cell spreading and matrix secretion (B). Seeded on COLs for seven days, ADSCs were cultured in adipogenic differentiation medium next. Lipid aggregations in ADSCs were visualized by Oil Red O staining gradually (C). The relative expression of adipogenic-specific genes, including PPAR-γ (D) and C-EBP (E). White arrows indicate cells and red arrows indicate matrix. Scale bars in A&C, 100 μm. Scale bars in B, 20 μm *p < 0.05, **p < 0.01.
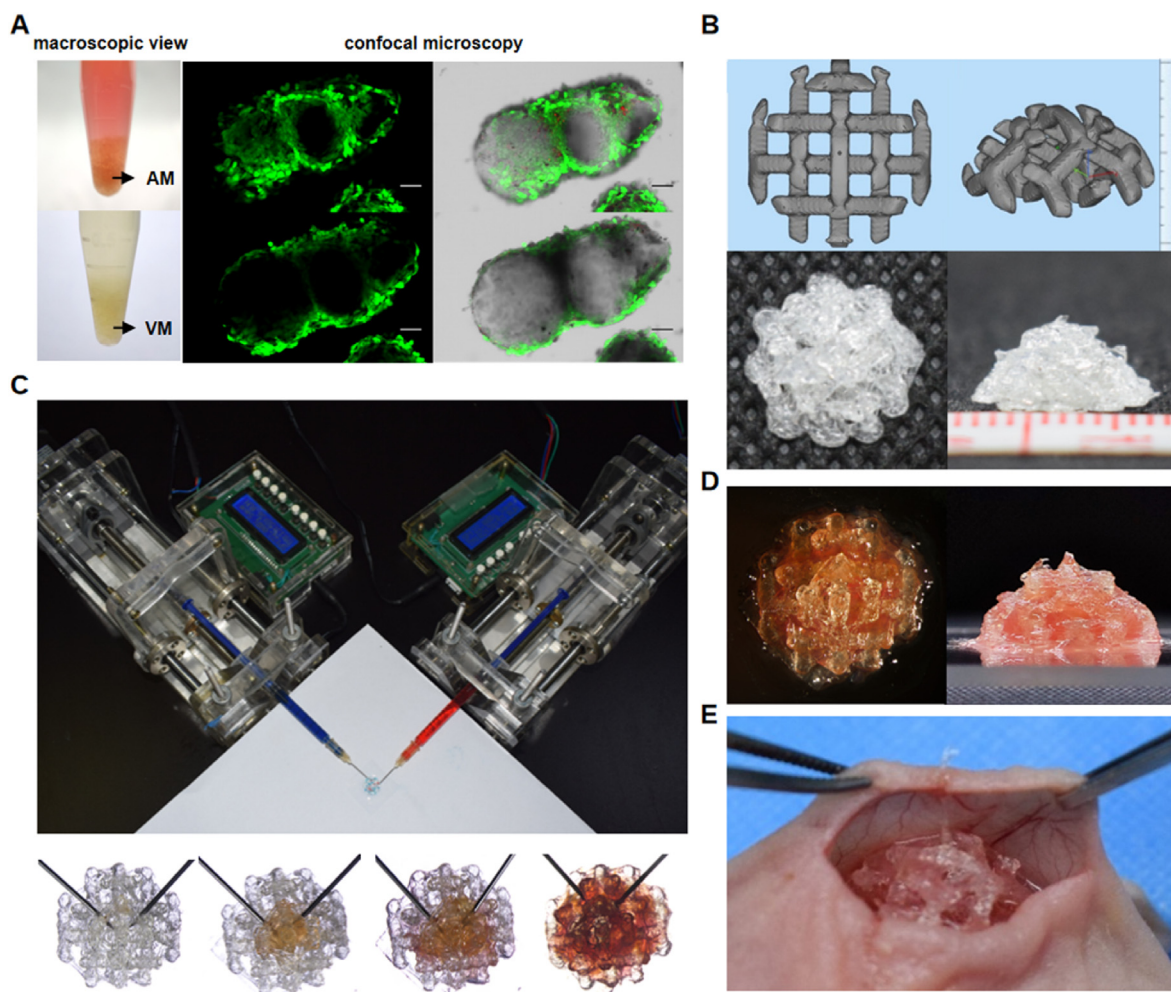
Fig. 4. Assembly of TEBG. After cell expansion for seven days and adipogenic induction for 14 d, AMs were collected. After cell expansion for seven days, VMs were collected. The macroscopic view and micro-tissues under confocal microscope (Middle: FITC. Right: merge of FITC, TRITC and TD.) were shown(A). The breast-like porous scaffold model was designed (B) and 3D printed with TPU (C). AMs and VMs were injected into the TPU scaffold and gradually filled the scaffold to full (D). The top view and cross-sectional view of TEBG were shown (E). TEBGs were transplanted under the dorsal skin of nude mice (F).

biocompatibility: First of all, collagen micro-droplets form continuously and steadily through the microfluidic technology with assistant of syringe pump and result in high throughput of collagen microgels. As Fig. 2B shown, collagen micro-droplets formed evenly in continuous oil phase due to constant shear force, with production efficiency as high as 400/min. Besides, microfluidics size is determined by the capillary inner diameter, liquid viscosity, smoothness of the pipeline and the flow rate ratio between the water and oil phases [34]. Thus, the diameter of COLs was adjusted by varying the flow rate ratio of the outward and inward layers in this study. COL with a diameter around 250 μm was adopted concerning that nutrients can diffuse only within ranges of 100–200 μm [35,36] and the size was proven to be uniform in Fig. 2D and I. Furthermore, the microgels composed of collagen met the requirements for highly compatible, cross-linkable and degradable biomaterials [37]. Collagen, as great content in natural ECM, has been well-recognized that it can facilitates cell adhesion, provide mechanical support for cells and mimic chemical microenvironment [38]. As illustrated in Fig. 3, ADSCs and HUVECs on COLs kept alive, gradually proliferated and reached a peak at d7. Additionally, collagen can be chemically crosslinked by EDC/NHS [39] into microgel, involving active carboxyl groups spontaneously bond to amine groups of lysine and hydroxylysine residues of collagen. This method results in collagen devices of good cytocompatibility and resistance to proteolytic attack [40], which prolongs collagen

degradation time. The COLs could be stored in vitro for more than a year and its degradation date was longer than 12weeks in vivo. In vivo HE results showed residual COLs (Fig. 5C).

The TEBG was fabricated by assembling AMs and VMs in 3D printed breast scaffold respectively, which was the novelty of this study and has the following advantages: 1) the injectable dual micro-tissues with controlled ratio and position could mimic the structure of native adipose tissue. Firstly, in adipose tissue, the fat lobule is the minimal essential unit and morphologically independent unit consisting of 100–1000 adipocytes and separated by fibrous septa and vessels. As adipocyte and endothelial cells are not connected to each other in adipose tissue, the ADSCs and HUVECs were cultured on COLs separately (Fig. 4A) and we cultured AMs in order to mimic fat lobules (Fig. 3C). During the separately cultivation of AMs and VMs in vitro, ADSCs or HUVECs were guaranteed in appropriate conditional medium, which facilitates cell proliferation, migration and differentiation. The high density of homogenous cells can facilitate cell-to-cell connection and matrix deposition. Therefore, by applying micro-tissues of different cell types as modules, the ratio of modules can be adjusted and modules can be assembled in various ways as needed. As Fig. 4D shown, the AMs and VMs were injectable and our injection method allowed for precise control of the micro-tissue content. A 1:1 ratio of AMs and VMs was adopted in this study to explore the effectiveness of dual micro-tissue strategy on
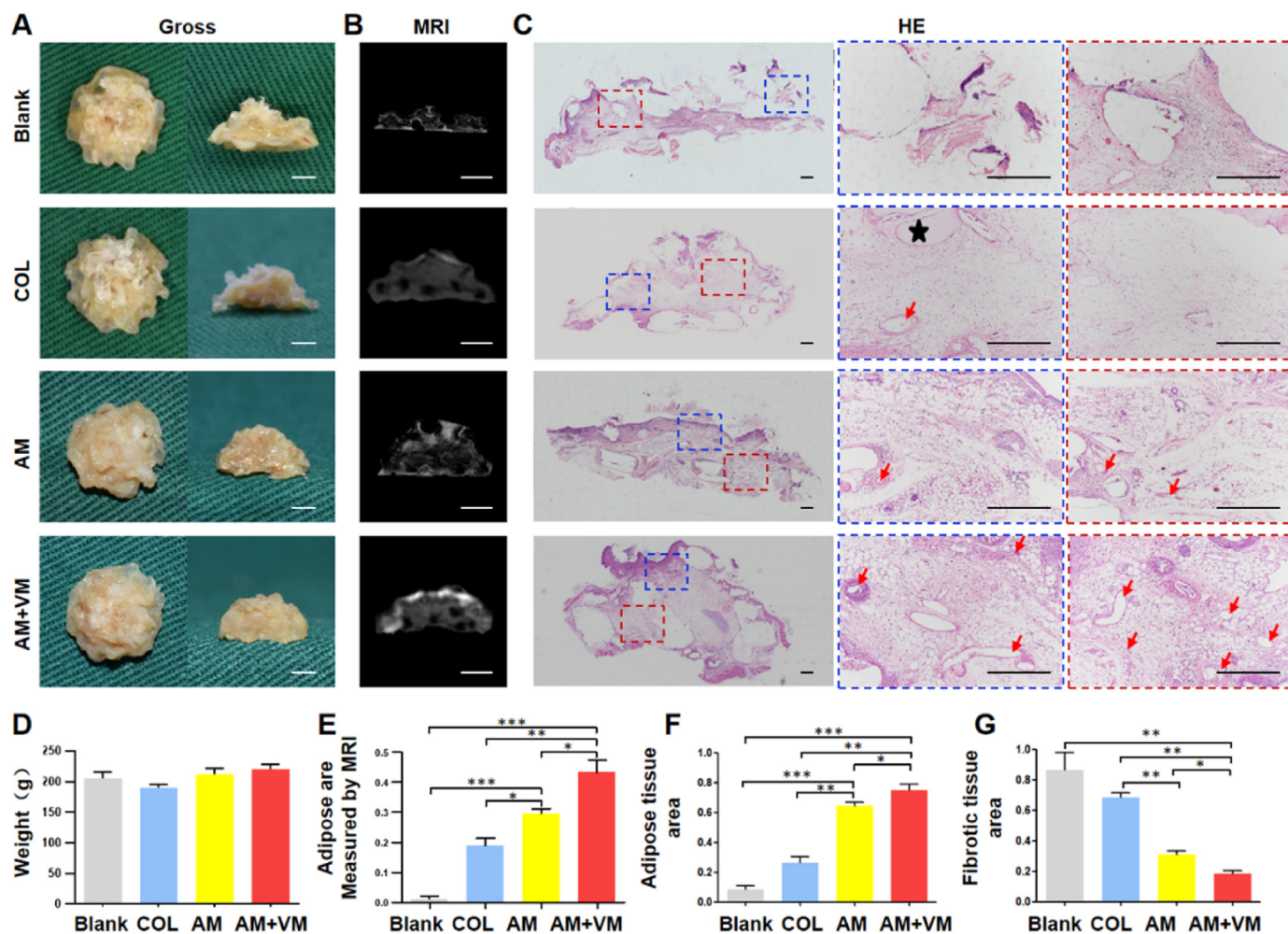
Fig. 5. Macroscopic view, Magnetic resonance imaging (MRI) and HE staining of explanted specimens 12 weeks after transplantation. Top view and cross-sectional view of TEBGs at 12 weeks (A). The weight of TEBGs among four groups have no statistic difference (D). MRI were taken to evaluate the adipose tissue volume. Adipose tissue was present with high signal at T1WI (B) and volume of adipose tissue was calculated (E). Overview and high magnification of HE cross-section (C). The adipose tissue area (F) and fibrotic tissue area (G) were calculated. Black star represents COL. The red arrows represent vessels. Scale bars, 100 μm. Bars represent the mean ± SD. *p < 0.05, **p < 0.01, ***p < 0.001.

lipogenesis and angiogenesis compared to strategy only using ADSCs micro-tissues, concerning that co-culturing ADSCs and HUVECs in a ratio of 50%:50% results in optimal osteogenesis and angiogenesis in bone tissue engineering [17,41]. Though Verseijden found a ratio of 1:5 (ADSCs: HUVECs) co-cultured in fibrin in vitro is better than 1:1 or 1:2 [27], the number of HUVECs on COL was more than ADSCs. The ratio of cells or micro-tissues and addition of micro-tissues composed of other cells such as breast epithelial cells may be explored to optimize multi-micro-tissues strategy in the future. 2) The 3D printed breast scaffold could mimic the mechanical property of native breast by improving its internal structure. In our previous research, breast scaffolds with various structures, similar to lattice structure, were manufactured and their mechanical properties were compared [42]. And the scaffold of N5S4 unit, which has 5 ordered arranged nodes and 4 interconnected struts (Fig. 4B and C), showed a compressive module similar to the natural breast [42]. Combined with delayed fat injection in vivo, the N5S4 exhibited higher fat volume retention, vascularization and less fibrosis, compared to stiffer scaffold. Thus, the N5S4 breast scaffold was adopted in the present study. The compression modules of breast-like TPU scaffold and the scaffold just assembled into TEBG had no significant difference. The TEBG of 12 weeks transplantation had higher compression module than just assembled (Fig. S5). The TPU scaffold was not degraded

in 12 weeks after implantation (Fig. 5C). Additionally, customization can be achieved to match the patient's breast defect through 3D printing.

The TEBG based on dual micro-tissues exhibited enhanced angiogenesis and adipogenesis in vivo. We speculate that this may be due to a reciprocal facilitation between AMs and VMs. According to various literature, tissue vessels are formed in two ways: from a precursor of endothelial cells or preexisting vessels by sprouting. The angiogenesis process may begin in the host cells, as shown in the Blank, COL, and AM groups lacking HUVECs. Compared to the Blank group and COL group, AM group and AM + VM group containing ADSCs has more CD31^{+} vessels for several possible reasons: On the one hand, ADSCs have multi-differentiation potential and could transform into endothelial cells and smooth muscle lineage in vivo [43]. Furthermore, factors secreted by ADSCs can induce endothelial cell proliferation and immigration to the central area. Additionally, the AM + VM group had the highest number of CD31 (+) vessels (Fig. 7B). This may be due to extra HUVECs on VMs spreading, assembling, and forming vessel in vivo. It is reported that HUVEC could form tubes when seeded on substrate especially matrigel and cultured in the appropriate conditional medium. It is reported that HUVECs supported by stem cells or human fibroblasts can form vessel structure [44]. The evidence suggests that injected HUVEC/collagen/alginate microspheres subcutaneously promoted angiogenesis in four
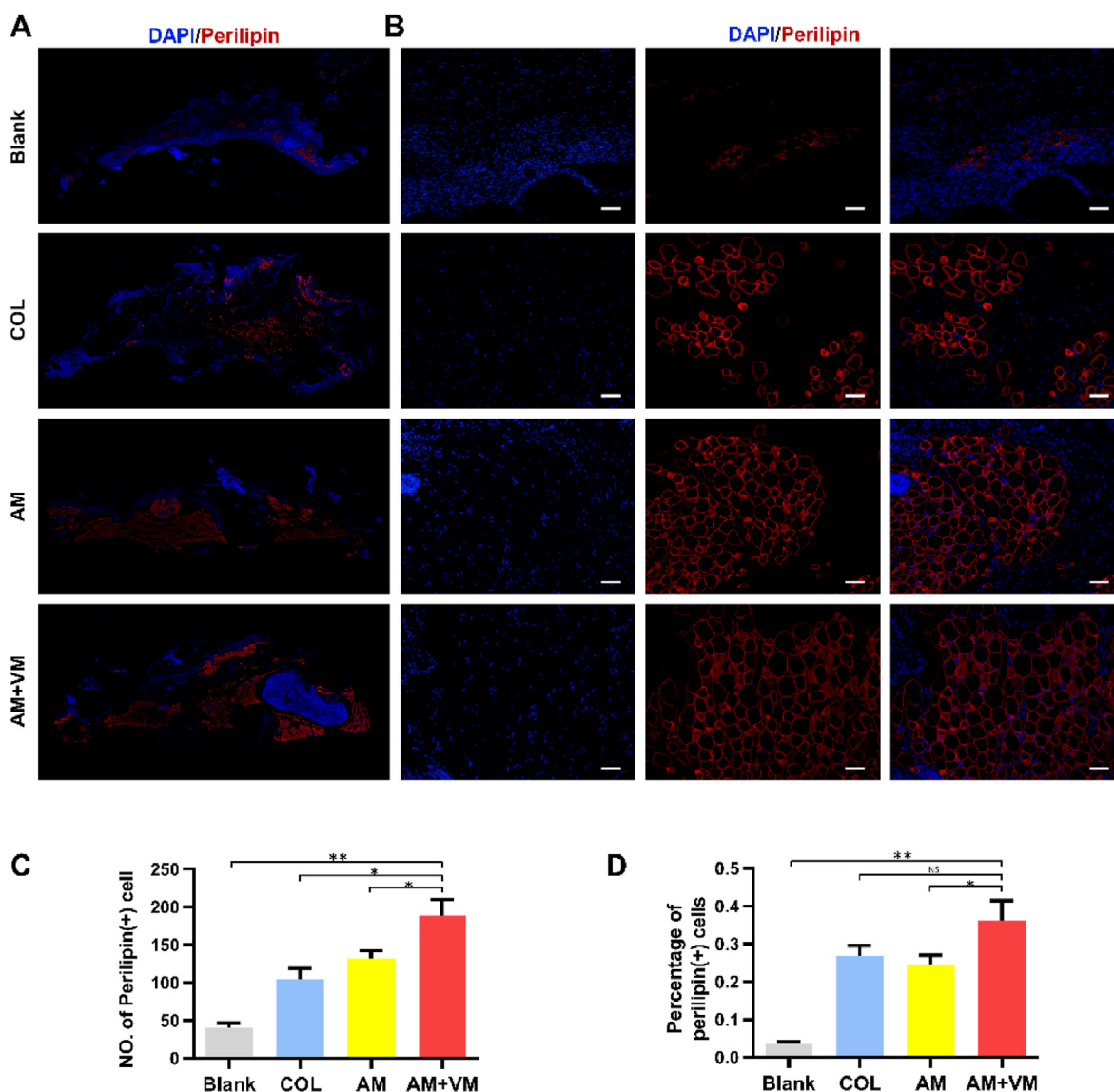
Fig. 6. Adipogenesis evaluation in vivo. Adipogenesis was evaluated by immunofluorescent localization of perilipin with red color (A). The lipid droplets in group AM + VM were circle and regular (B). The number of perilipin (+) cells and the percentage of perilipin (+) cells in group AM + VM were largest in four groups (C, D). Scale bars, 100 μm. Bars represent the mean ± SD. $*p < 0.05$, $**p < 0.01$, $***p < 0.001$.

weeks [31]. Similarly, in our study, human and mouse-derived CD31 (+) cells indicate vessel formation by injecting HUVECs, and host vessels grow into the outer region (Fig. S6). In the end, both human and mouse-derived vessels are merged and connected. Smooth muscle cells derived from mouse surrounded HUVEC-lumen and stabilized them (Fig. S7). At last, the neovascularization enhanced adipogenesis through increased nutrient perfusion and recruitment of in situ cells through the blood vessels.

Micro-tissues engineering for adipose/breast have been explored by several groups. Most of them constructed adipose-like micro-tissues in vitro [19,45]. Hoefner, C cultured self-assembly ADSC spheroids using the liquid overlay technique and evaluated the ECM of differentiated ADSC spheroids, which was proved to be similar to native adipose [17]. Colle, J A encapsulated ADSC spheroids in methacrylated gelatin (GelMA) ink and combined it with 3D printing to prepare scaffold. Though the RT-qPCR of ADSC spheroids in GelMA ink was performed, adipogenesis was not observed and experiment in vivo was not done [46]. Team of Yao applied micro-tissues in vivo. Yao prepared collagen/alginate hydrogel microsphere for ADSCs embedding and adipogenic

differentiation in vitro. The microspheres were injected subcutaneously into head of nude mice and generated vascularized adipose tissue in vivo after 4 weeks [18]. Compared to Yao, we applied dual micro-tissues and verify the adipogenesis and angiogenesis of dual micro-tissues strategy (AM + VM group) was significantly better than only ADSC micro-tissues strategy (AM group), which Yao's method could be also classified into. Later, Yao's team prepared differentiated ADSCs/collagen/alginate microspheres surface-coated HUVECs and injected them subcutaneously [31]. It seems that we both adopted ADSCs and HUVECs to construct micro-tissues for vascularized adipose regeneration in vivo, there were still obvious differences between our researches. The novelty of this study is culturing dual micro-tissues separately as building block and assembled them immediately before transplantation, which presented excellent regeneration in vivo. Firstly, separate cultivation of AMs and VMs in vitro guaranteed cells in appropriate conditional medium in simple and easy way, while the co-culture conditions of ADSCs and HUVECs allowing for simultaneous survival and function of both cells were elusive and complex. It is found that vital components in adipogenic differentiation medium such as IBMX would inhibit HUVEC proliferation
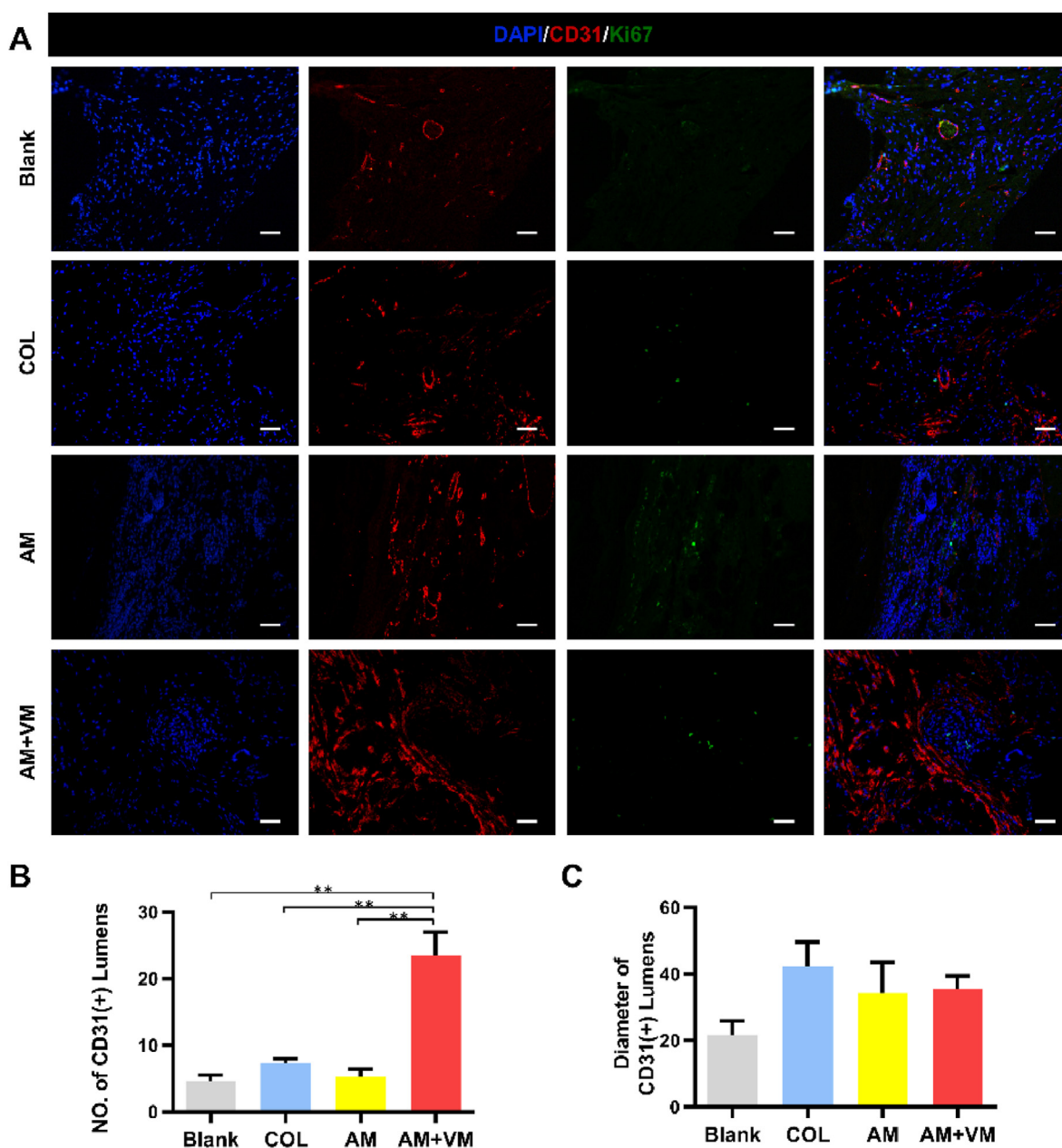
Fig. 7. Angiogenesis evaluation in vivo. CD31 immunofluorescence staining was performed to identify vascular endothelial cells and ki67 staining was marked with green fluorescence to identify cells with proliferation capacity (A). AM + VM group had largest number of CD31 (+) lumens in all groups (B). The average diameter of CD31 (+) lumens had no statistic difference in all groups (C). Scale bars, 100 μm *p < 0.05, **p < 0.01, ***p < 0.001.

[47], and components in endothelial cell media such as EGF and hydrocortisone inhibited adipogenic differentiation and exhibit lipolytic activities [48]. Secondly, the dual micro-tissues strategy makes it possible to change the ratio and position of different micro-tissues in the future. Thirdly, the dual micro-tissues strategy presented excellent vascularized adipose regeneration and lay groundwork for multi-microtissues engineered breast.

5. Conclusions

The current study has demonstrated that developing AMs (based on ADSCs) and VMs (based on HUVECs) as dual building blocks and assembling them can result in vascularized adipose tissue in a nude mouse model. Besides, the collagen microspheres fabricated using a microfluidic chip are appropriate carriers for ADSCs and HUVECs. The present study lays the groundwork for future research in larger sized bottom-up breast tissue engineering and construction of heterogeneous tissue based on multi-component building blocks.

Data available statement

The raw data are available from corresponding author upon reasonable request.

Credit author statement

Ruopiao Ni: Investigation, Formal analysis, Data curation, Visualization, Writing - Original Draft. **Chao Luo:** Investigation, Writing - Review & Editing. **Hai Ci:** Investigation. **Di Sun:** Writing - Review & Editing. **Ran An:** Funding acquisition. **Zhenxing Wang:** Conceptualization, Supervision, Writing - Review & Editing. **Jie Yang:** Funding acquisition. **Yiqing Li:** Project administration. **Jiaming Sun:** Project

administration, Funding acquisition.

Declaration of competing interest

The authors declare that they have no known competing financial interests or personal relationships that could have appeared to influence the work reported in this paper.

Data availability

Data will be made available on request.

Acknowledgments

Appendix A. Supplementary data

Supplementary data to this article can be found online at https://doi.org/10.1016/j.mtbio.2022.100539.

References

[1] C.J. Coroneos, et al., US FDA breast implant postapproval studies: long-term outcomes in 99,993 patients, Ann. Surg. 269 (1) (2019) 30–36.
[2] G.K. Lee, C.C. Sheckter, Breast reconstruction following breast cancer treatment-2018, JAMA 320 (12) (2018) 1277–1278.
[3] C. Conci, et al., Tissue engineering and regenerative medicine strategies for the female breast, J. Tissue Eng. Regen. Med. 14 (2) (2020) 369–387.
[4] L. Wang, et al., Combining decellularized human adipose tissue extracellular matrix and adipose-derived stem cells for adipose tissue engineering, Acta Biomater. 9 (11) (2013) 8921–8931.
[5] C. Yu, et al., Porous decellularized adipose tissue foams for soft tissue regeneration, Biomaterials 34 (13) (2013) 3290–3302.
[6] J.M. Sobral, et al., Three-dimensional plotted scaffolds with controlled pore size gradients: effect of scaffold geometry on mechanical performance and cell seeding efficiency, Acta Biomater. 7 (3) (2011) 1009–1018.
[7] J. Huling, et al., Fabrication of biomimetic vascular scaffolds for 3D tissue constructs using vascular corrosion casts, Acta Biomater. 32 (2016) 190–197.
[8] T. Kaully, et al., Vascularization–the conduit to viable engineered tissues, Tissue Eng. B Rev. 15 (2) (2009) 159–169.
[9] D.L. Elbert, Bottom-up tissue engineering, Curr. Opin. Biotechnol. 22 (5) (2011) 674–680.
[10] N. Tejavibulya, et al., Directed self-assembly of large scaffold-free multi-cellular honeycomb structures, Biofabrication 3 (3) (2011), 034110.
[11] C. Luo, et al., Biomimetic open porous structured core-shell microtissue with enhanced mechanical properties for bottom-up bone tissue engineering, Theranostics 9 (16) (2019) 4663–4677.
[12] K.M. Kennedy, A. Bhaw-Luximon, D. Jhurry, Cell-matrix mechanical interaction in electrospun polymeric scaffolds for tissue engineering: implications for scaffold design and performance, Acta Biomater. 50 (2017) 41–55.
[13] J.L. Madrigal, et al., Microgels produced using microfluidic on-chip polymer blending for controlled released of VEGF encoding lentivectors, Acta Biomater. 69 (2018) 265–276.
[14] R. Gauvin, et al., Hydrogels and microtechnologies for engineering the cellular microenvironment, Wiley Interdiscip. Rev. Nanomed. Nanobiotechnol. 4 (3) (2012) 235–246.
[15] T. Sun, et al., Engineered tissue micro-rings fabricated from aggregated fibroblasts and microfibres for a bottom-up tissue engineering approach, Biofabrication 11 (3) (2019), 035029.
[16] N. Naderi, et al., The regenerative role of adipose-derived stem cells (ADSC) in plastic and reconstructive surgery, Int. Wound J. 14 (1) (2017) 112–124.
[17] C. Hoefner, et al., Human adipose-derived mesenchymal stromal/stem cell spheroids possess high adipogenic capacity and acquire an adipose tissue-like extracellular matrix pattern, Tissue Eng. 26 (15–16) (2020) 915–926.
[18] R. Yao, et al., Injectable cell/hydrogel microspheres induce the formation of fat lobule-like microtissues and vascularized adipose tissue regeneration, Biofabrication 4 (4) (2012), 045003.
[19] M. Lago, et al., Generation of gellan gum-based adipose-like microtissues, Bioengineering 5 (3) (2018).
[20] P. Xia, et al., Injectable stem cell laden open porous microgels that favor adipogenesis: in vitro and in vivo evaluation, ACS Appl. Mater. Interfaces 9 (40) (2017) 34751–34761.
[21] C.W. Patrick, Breast tissue engineering, Annu. Rev. Biomed. Eng. 6 (1) (2004) 109–130.
[22] H. Eto, et al., Characterization of structure and cellular components of aspirated and excised adipose tissue, Plast. Reconstr. Surg. 124 (4) (2009) 1087–1097.
[23] S.T. Kølle, et al., Enrichment of autologous fat grafts with ex-vivo expanded adipose tissue-derived stem cells for graft survival: a randomised placebo-controlled trial, Lancet 382 (9898) (2013) 1113–1120.
[24] P. Gangadaran, et al., Identification of angiogenic cargo in extracellular vesicles secreted from human adipose tissue-derived stem cells and induction of angiogenesis in vitro and in vivo, Pharmaceutics 13 (4) (2021).
[25] J. Colle, et al., Bioprinting predifferentiated adipose-derived mesenchymal stem cell spheroids with methacrylated gelatin ink for adipose tissue engineering, J. Mater. Sci. Mater. Med. 31 (4) (2020) 36.
[26] F. Verseijden, et al., Prevascular structures promote vascularization in engineered human adipose tissue constructs upon implantation, Cell Transplant. 19 (8) (2010) 1007–1020.
[27] F. Verseijden, et al., Vascularization of prevascularized and non-prevascularized fibrin-based human adipose tissue constructs after implantation in nude mice, J. Tissue Eng. Regen. Med. 6 (3) (2012) 169–178.
[28] A. Freiman, et al., Adipose-derived endothelial and mesenchymal stem cells enhance vascular network formation on three-dimensional constructs in vitro, Stem Cell Res. Ther. 7 (2016) 5.
[29] J. Ma, et al., In vitro and in vivo angiogenic capacity of BM-MSCs/HUVECs and AT-MSCs/HUVECs cocultures, Biofabrication 6 (1) (2014), 015005.
[30] J.R. Sarkanen, et al., Adipose stromal cell tubule network model provides a versatile tool for vascular research and tissue engineering, Cells Tissues Organs 196 (5) (2012) 385–397.
[31] R. Yao, et al., Biomimetic injectable HUVEC-adipocytes/collagen/alginate microsphere co-cultures for adipose tissue engineering, Biotechnol. Bioeng. 110 (5) (2013) 1430–1443.
[32] M.J. Susienka, B.T. Wilks, J.R. Morgan, Quantifying the kinetics and morphological changes of the fusion of spheroid building blocks, Biofabrication 8 (4) (2016), 045003.
[33] D. Bezuidenhout, D.F. Williams, P. Zilla, Polymeric heart valves for surgical implantation, catheter-based technologies and heart assist devices, Biomaterials 36 (2015) 6–25.
[34] D. Liu, et al., Microfluidic-assisted fabrication of carriers for controlled drug delivery, Lab Chip 17 (11) (2017) 1856–1883.
[35] R.J. McMurtrey, Roles of diffusion dynamics in stem cell signaling and three-dimensional tissue development, Stem Cell. Dev. 26 (18) (2017) 1293–1303.
[36] J. Liu, et al., Monitoring nutrient transport in tissue-engineered grafts, J. Tissue Eng. Regen. Med. 9 (8) (2015) 952–960.
[37] M. Nie, S. Takeuchi, Bottom-up biofabrication using microfluidic techniques, Biofabrication 10 (4) (2018), 044103-044103.
[38] L.C. Massimino, et al., Use of Collagen and Auricular Cartilage in Bioengineering: Scaffolds for Tissue Regeneration, Cell Tissue Bank, 2020.
[39] M. Nair, et al., Tunable bioactivity and mechanics of collagen-based tissue engineering constructs: a comparison of EDC-NHS, genipin and TG2 crosslinkers, Biomaterials 254 (2020), 120109.
[40] A. Sorushanova, et al., The collagen suprafamily: from biosynthesis to advanced biomaterial development, Adv. Mater. 31 (1) (2019) e1801651.
[41] J. Ma, et al., Adipose tissue-derived mesenchymal stem cells as monocultures or cocultures with human umbilical vein endothelial cells: performance in vitro and in rat cranial defects, J. Biomed. Mater. Res. 102 (4) (2014) 1026–1036.
[42] M. Zhou, et al., Tuning the mechanics of 3D-printed scaffolds by crystal lattice-like structural design for breast tissue engineering, Biofabrication 12 (1) (2020), 015023.
[43] W. Gu, et al., Single-cell RNA-sequencing and metabolomics analyses reveal the contribution of perivascular adipose tissue stem cells to vascular remodeling, Arterioscler. Thromb. Vasc. Biol. 39 (10) (2019) 2049–2066.
[44] L. De Moor, et al., High-throughput fabrication of vascularized spheroids for bioprinting, Biofabrication 10 (3) (2018), 035009.
[45] F. Yang, et al., A 3D human adipose tissue model within a microfluidic device, Lab Chip 21 (2) (2021) 435–446.
[46] J. Colle, et al., Bioprinting predifferentiated adipose-derived mesenchymal stem cell spheroids with methacrylated gelatin ink for adipose tissue engineering, J. Mater. Sci. Mater. Med. 31 (4) (2020) 36.
[47] F. Yang, R.N. Cohen, E.M. Brey, Optimization of Co-culture conditions for a human vascularized adipose tissue model, Bioengineering 7 (3) (2020).
[48] A.C. Volz, et al., EGF and hydrocortisone as critical factors for the co-culture of adipogenic differentiated ASCs and endothelial cells, Differentiation 95 (2017) 21–30.